Draft version January 14, 2022
Typeset using LaTeX/show your work! modern style in AASTeX631

# What can we learn about exoplanet maps in emitted light from photometric observations of secondary eclipses using JWST?

Fran Bartolić,[1,2] Rodrigo Luger,[2] and Daniel Foreman-Mackey[2]

[1] Centre for Exoplanet Science, SUPA, School of Physics and Astronomy, University of St. Andrews, St. Andrews, UK

[2] Center for Computational Astrophysics, Flatiron Institute, New York, NY, USA

## ABSTRACT

We investigate the degeneracies involved in the process of reconstructing spatial maps of exoplanets from secondary eclipse light curves in emitted light, and test the feasibility of spatially resolving localized features on the daysides of Hot Jupiters using JWST. We find that even with noiseless light curves and assuming fixed orbital parameters, there are interesting degeneracies in the structure of inferred maps. With realistic light curves, differentiating between a homogenous spot and finer spatial structure (due to, for instance, the presence of large storms and clouds) is highly dependant on the intensity contrast between the feature and the background. There is a signal-to-noise dependent threshold which needs to be reached so that the ingress and egress parts of the light curve start constraining higher order modes of the surface map. Without reaching this threshold there is no hope of constraining finer structure on the dayside of the planet and the information content about the surface is dominated by the phase curve signal and the eclipse depth. We find that even for the brightest Hot Jupiters, the signal-to-noise ratio of the simulated JWST light curves isn't high enough to provide much information about the surface beyond excluding the presence of very high contrast features.

## 1. INTRODUCTION

One of the most notable advances in exoplanetary science over the past decade has been the ability to reconstruct coarse two-dimensional spatial maps of exoplanets using high precision phase curves and secondary eclipse observations. Knutson et al. (2007), Majeau et al. (2012) and de Wit et al. (2012) used Spitzer mid-infrared observations of secondary eclipses of the Hot Jupiter HD189733b and found that surface emission is best described by the presence of a large hot spot on the dayside of the planet which is longitudinally offset from the substellar point. Similarly, Stevenson et al. (2014) produced temperature maps of the Hot Jupiter WASP-43b, Demory et al. (2013) mapped the Hot Jupiter Kepler-7b in reflected light and Demory et al. (2016)

fb90@st-andrews.ac.uk

mapped the thermal emission from the Super Earth 55 Cancri e, although all of these only captured longitudinal variations in intensity.

Real exoplanet atmospheres of are certain to have three-dimensional spatial inhomogeneities in emission more complex than a single hot spot due to the presence of clouds, zonal jets, storms, waves etc. (Showman et al. 2020). Recent high resolution simulations of Hot Jupiter atmospheres by Cho et al. (2021) which were able to capture smaller scale turbulence show the presence of storms at a range of scales, including planetary scales, with quasi-periodic time variability and multiple equilibrium cycles. These atmospheric phenomena should result in spatial variation in the intensity of emitted and reflected light across the visible disc of the planet which is potentially observable.

There have been significant advances in statistical modeling of phase curves and eclipse light curves in recent years. Most notably, Luger et al. (2019) introduced the `starry` algorithm which enables analytic computation of phase curves and occultation light curves for bodies with arbitrary emission maps expressed in a spherical harmonic basis andLuger et al. (2021) expanded the algorithm for the (considerably more complicated) case of reflected light.

of bodies whose emission surface is expanded in a basis of spherical harmonics.

In this paper, we investigate under which conditions it possible to recover more complex spatial features than large hot spots. We focus on emitted light from tidally locked planets and ignore uncertainties in the orbital elements. We start by describing the degeneracies inherent in the eclipse mapping problem even at infinite signal-to-noise and then investigate the relationship between noise and information content of phase curves and eclipse light curves.

## 2. METHODS

### 2.1. *Model*

We use the `starry` mapping framework (CITE) to compute eclipse light curves of a simulated planet with thermal surface emission. `starry` enables fast computation of occultation (eclipse) light curves in both emitted and reflected light by analytically integrating the flux over the planet and the stellar disc Most importantly, `starry`

To compute eclipse light curves

## 3. RESULTS

### 3.1. *Degeneracies*

## 4. DISCUSSION

## REFERENCES


Cho, J. Y.-K., Skinner, J. W., & Thrastarson, H. T. 2021, arXiv:2105.12759 [astro-ph]. https://arxiv.org/abs/2105.12759

de Wit, J., Gillon, M., Demory, B.-O., & Seager, S. 2012, A&A, 548, A128, doi: 10.1051/0004-6361/201219060

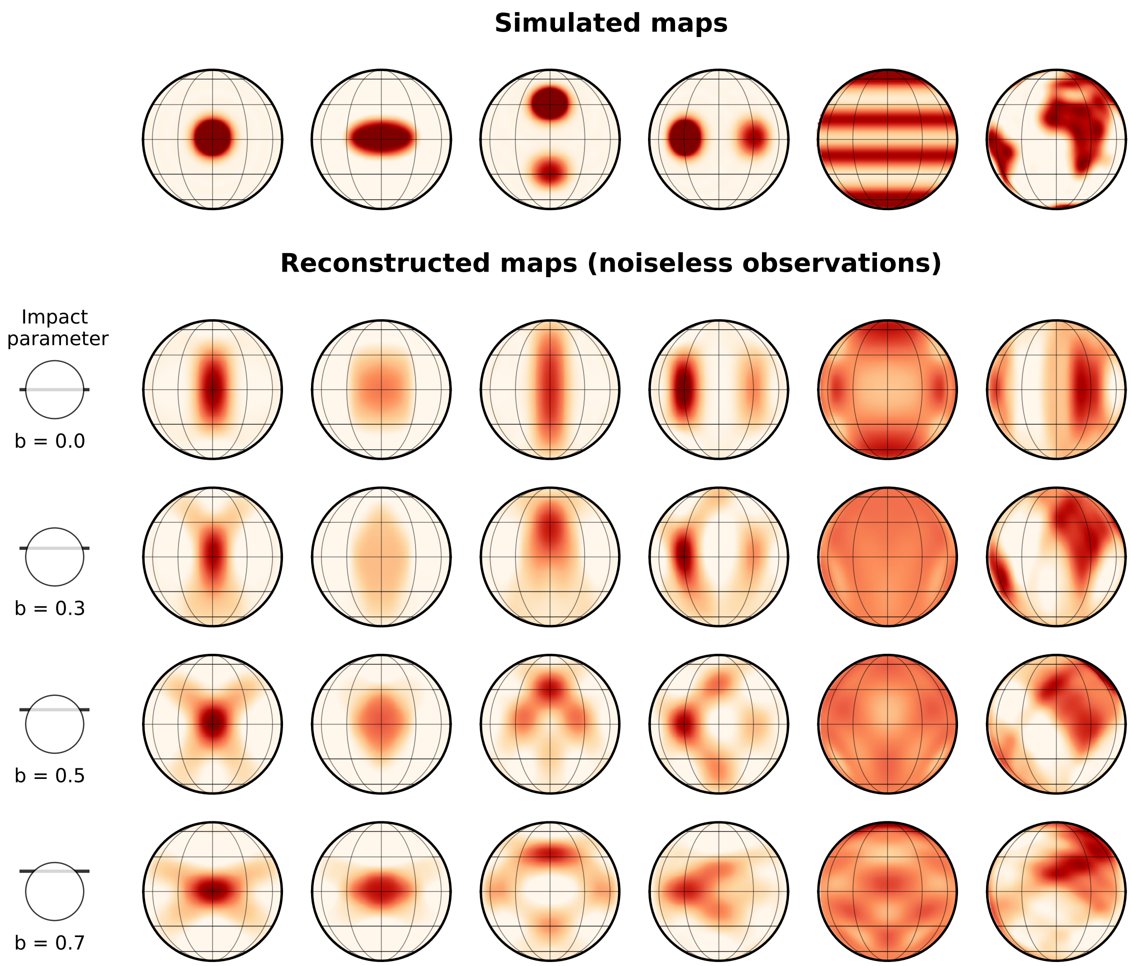


**Figure 1.**


Demory, B.-O., de Wit, J., Lewis, N., et al. 2013, The Astrophysical Journal, 776, L25, doi: 10.1088/2041-8205/776/2/L25

Demory, B.-O., Gillon, M., de Wit, J., et al. 2016, Nature, 532, 207, doi: 10.1038/nature17169

Knutson, H. A., Charbonneau, D., Allen, L. E., et al. 2007, Nature, 447, 183, doi: 10.1038/nature05782

Luger, R., Agol, E., Bartolić, F., & Foreman-Mackey, D. 2021, Analytic Light Curves in Reflected Light: Phase Curves, Occultations, and Non-Lambertian Scattering for Spherical Planets and Moons

Luger, R., Agol, E., Foreman-Mackey, D., et al. 2019, The Astronomical Journal, 157, 64, doi: 10.3847/1538-3881/aae8e5

Majeau, C., Agol, E., & Cowan, N. B. 2012, The Astrophysical Journal Letters, 747, L20, doi: 10.1088/2041-8205/747/2/L20

Showman, A. P., Tan, X., & Parmentier, V. 2020, Space Sci Rev, 216, 139, doi: 10.1007/s11214-020-00758-8

Stevenson, K. B., Désert, J.-M., Line, M. R., et al. 2014, Science, 346, 838, doi: 10.1126/science.1256758

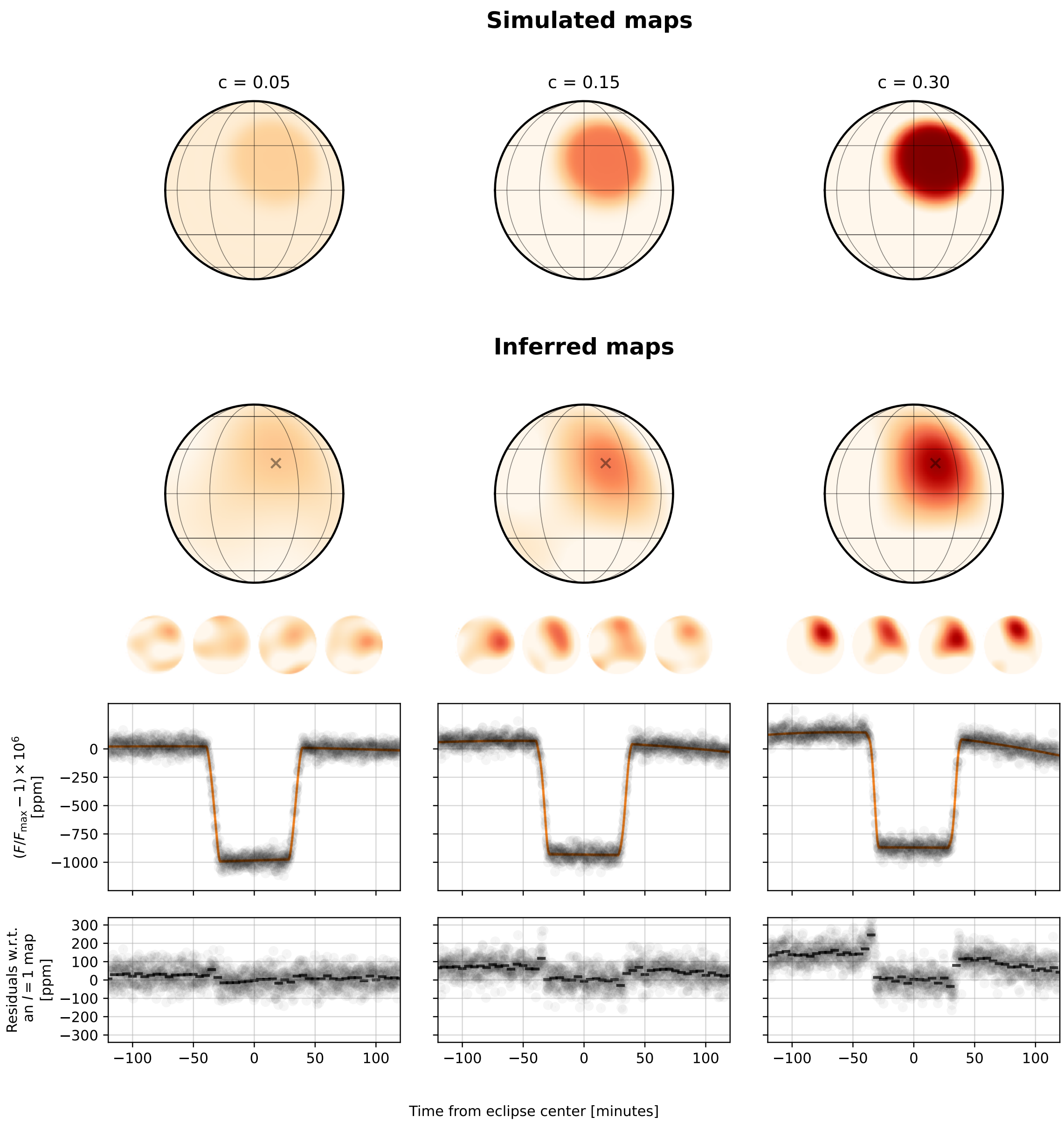


**Figure 2.**

# APPENDIX

## A. APPENDIX 1

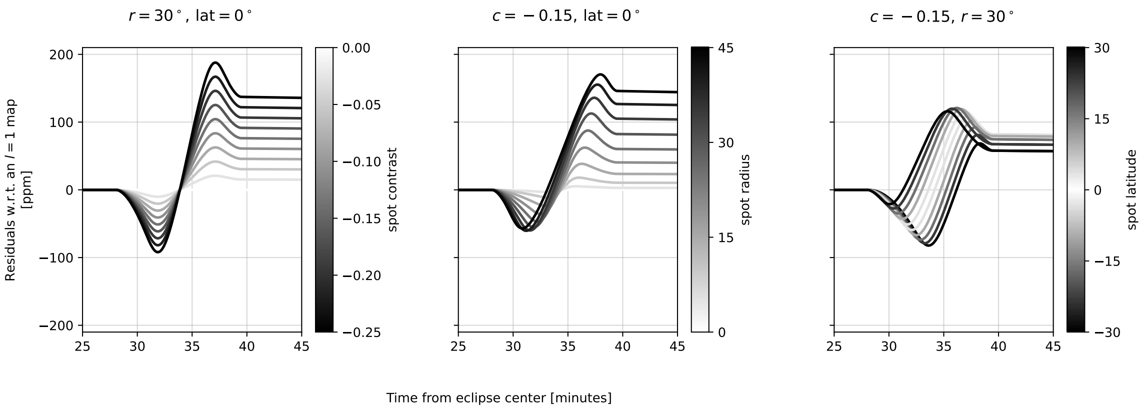


**Figure 3.**

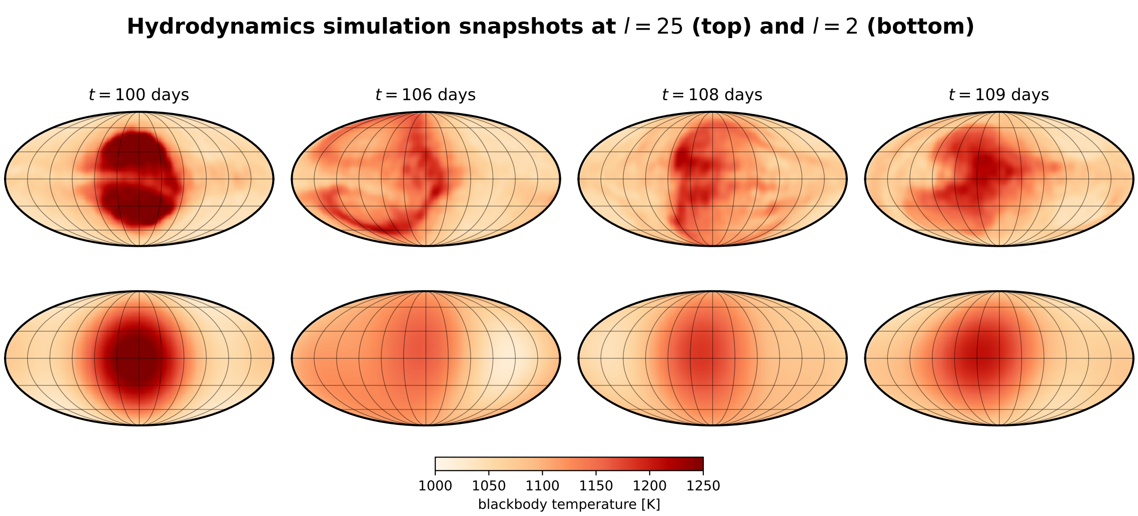


**Figure 4.**

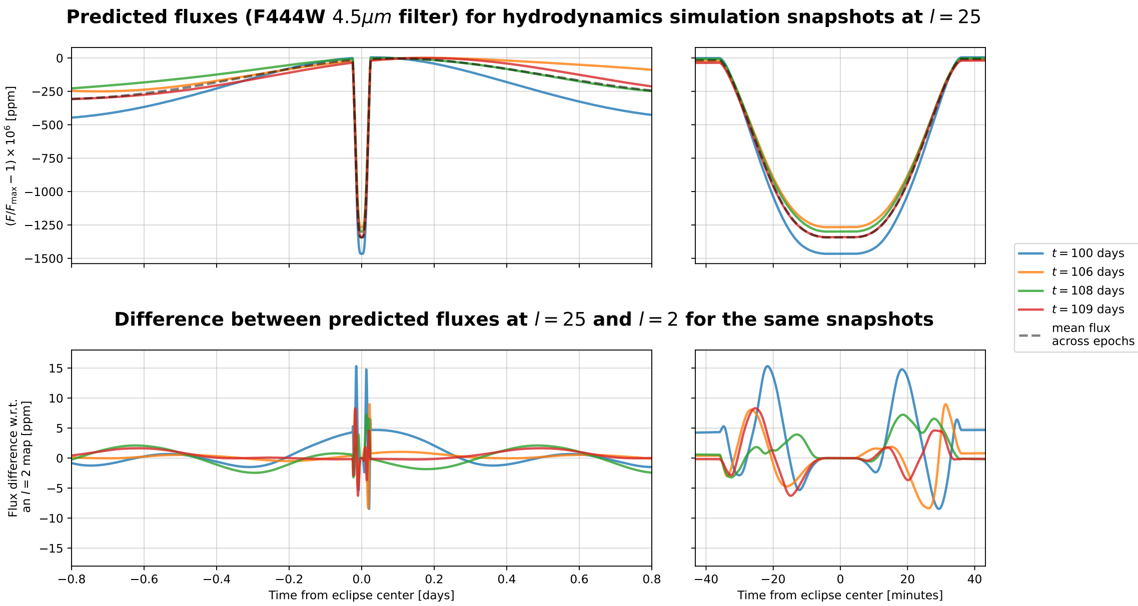

Predicted fluxes (F444W 4.5$\mu m$ filter) for hydrodynamics simulation snapshots at $l = 25$
$(F/F_{\max} - 1) \times 10^6$ [ppm]
Difference between predicted fluxes at $l = 25$ and $l = 2$ for the same snapshots
Flux difference w.r.t. an $l = 2$ map [ppm]
Time from eclipse center [days]
Time from eclipse center [minutes]
$t = 100$ days
$t = 106$ days
$t = 108$ days
$t = 109$ days
mean flux across epochs


**Figure 5.**

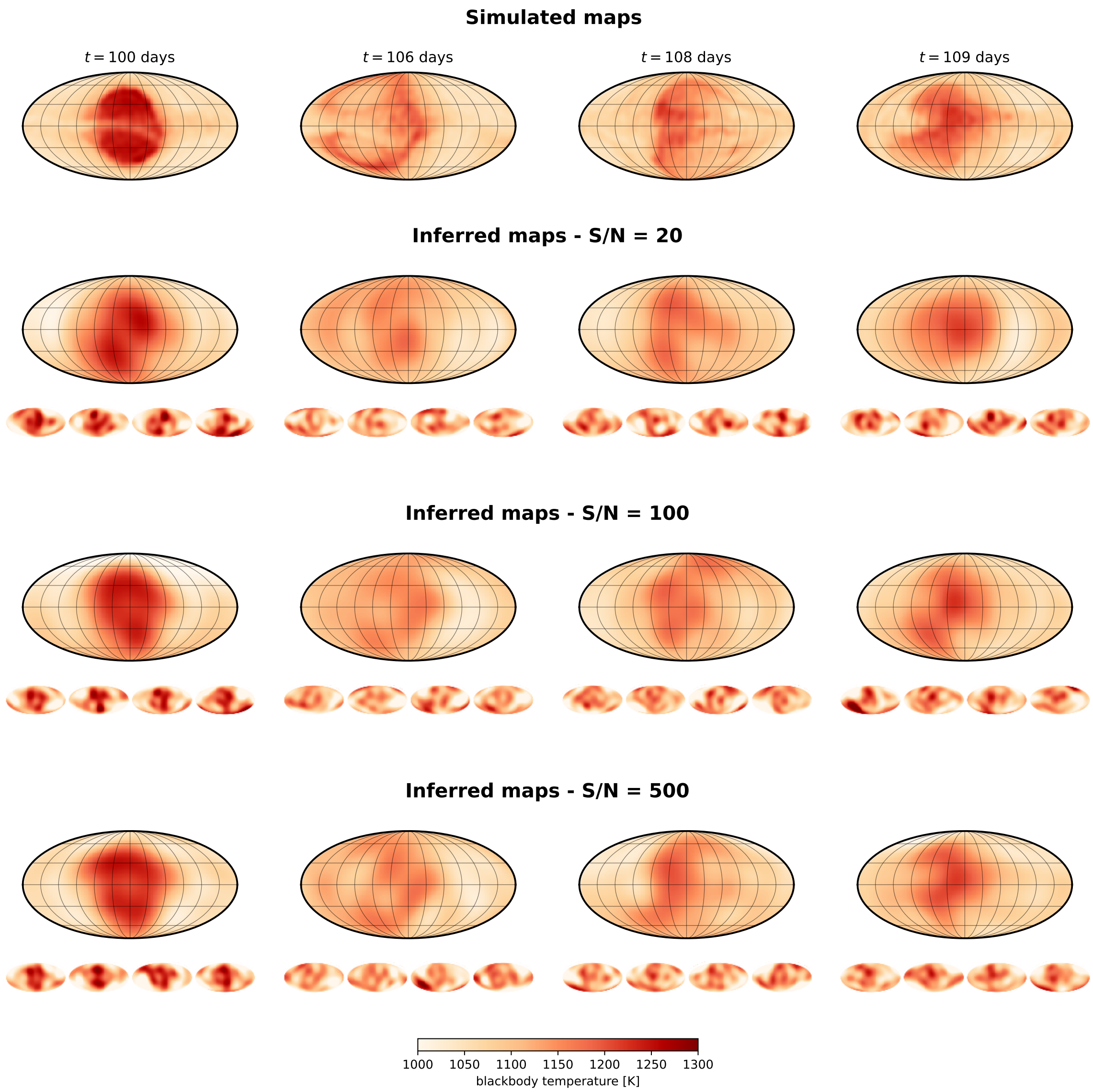
Simulated maps
$t = 100$ days
$t = 106$ days
$t = 108$ days
$t = 109$ days
Inferred maps - S/N = 20
Inferred maps - S/N = 100
Inferred maps - S/N = 500
1000
1050
1100
1150
1200
1250
1300
blackbody temperature [K]

**Figure 6.**